



BNL-96472-2011-CP

***Resonant Soft X-ray Scattering Studies of
Multiferroic YMn_2O_5***

**S. Partzsch^{1,2}, S. B. Wilkins², E. Schierle³, V. Soltwisch³,
J. P. Hill², E. Weschke³, D. Souptel¹, B. Buchner¹, and J. Geck¹**

¹Leibniz Institute for Solid State and Materials Research IFW Dresden,
Helmholtzstrasse 20, 01069 Dresden, Germany

²Condensed Matter Physics and Material Science Department, Brookhaven
National Laboratory, Upton, New York, 11973 USA

³Helmholtz-Zentrum Berlin für Materialien und Energie, Albert-Einstein-Str.
15, 12489 Berlin, Germany

Presented at the REXS 2011 Conference
In Aussois, France
June 17, 2011

October 2011

Condensed Matter Physics & Materials Science Department

Brookhaven National Laboratory

**U.S. Department of Energy
DOE - OFFICE OF SCIENCE**

Notice: This manuscript has been authored by employees of Brookhaven Science Associates, LLC under Contract No. DE-AC02-98CH10886 with the U.S. Department of Energy. The publisher by accepting the manuscript for publication acknowledges that the United States Government retains a non-exclusive, paid-up, irrevocable, world-wide license to publish or reproduce the published form of this manuscript, or allow others to do so, for United States Government purposes.

This preprint is intended for publication in a journal or proceedings. Since changes may be made before publication, it may not be cited or reproduced without the author's permission.

DISCLAIMER

This report was prepared as an account of work sponsored by an agency of the United States Government. Neither the United States Government nor any agency thereof, nor any of their employees, nor any of their contractors, subcontractors, or their employees, makes any warranty, express or implied, or assumes any legal liability or responsibility for the accuracy, completeness, or any third party's use or the results of such use of any information, apparatus, product, or process disclosed, or represents that its use would not infringe privately owned rights. Reference herein to any specific commercial product, process, or service by trade name, trademark, manufacturer, or otherwise, does not necessarily constitute or imply its endorsement, recommendation, or favoring by the United States Government or any agency thereof or its contractors or subcontractors. The views and opinions of authors expressed herein do not necessarily state or reflect those of the United States Government or any agency thereof.

EPJ manuscript No.
(will be inserted by the editor)

Resonant Soft X-ray Scattering Studies of Multiferroic YMn_2O_5

S. Partzsch^{1,2}, S. B. Wilkins², E. Schierle³, V. Soltwisch³, J. P. Hill², E. Weschke³, D. Souptel¹, B. Büchner¹, and J. Geck¹

¹ Leibniz Institute for Solid State and Materials Research IFW Dresden, Helmholtzstrasse 20, 01069 Dresden, Germany

² Condensed Matter Physics and Material Science Department, Brookhaven National Laboratory, Upton, New York, 11973 USA

³ Helmholtz-Zentrum Berlin für Materialien und Energie, Albert-Einstein-Str.15, 12489 Berlin, Germany

Abstract. We performed soft x-ray resonant scattering at the Mn $L_{2,3}$ - and O K edges of YMn_2O_5 . While the resonant intensity at the Mn $L_{2,3}$ edges represent the magnetic order parameter, the resonant scattering at the O K edge is found to be directly related to the macroscopic ferroelectric polarization. The latter observation reveals the important role of the spin-dependent Mn-O hybridization for the multiferroicity of YMn_2O_5 . We present details about how to obtain correct energy dependent lineshapes and discuss the origin of the resonant intensity at the O K edge.

1 Introduction

Multiferroic materials gained a lot of attention for their possible applications like magnetic computer memory which is switched by electrical fields (see, e. g., [1,2]). Transition metal oxide compounds realize a number of frustrated magnetic materials [3,4], where the ferroelectric (FE) polarization, \mathcal{P} , is driven by magnetic ordering. Hence they have a large magneto-electric (ME) coupling.

The origin of this ME coupling was first explained by distortions of the ionic lattice, which optimize the energy of the magnetic system by modulations of the ionic positions of Mn and/or O (\mathcal{P}_{ion}) [1–4]. Recently another contribution to the polarization, i. e., one due to the valence electrons (\mathcal{P}_{el}) of Mn and O, has been discussed by theory [5–7] and observed by resonant soft x-ray scattering (RSXS) [8]. Other indications for \mathcal{P}_{el} from experiments can be found in [9,10].

In YMn_2O_5 manganese occupies two different crystallographic sites; the first coordinated by an oxygen octahedron (Mn1) and the second by an oxygen square-based pyramid (Mn2) [11,12]. The Mn1-octahedra form edge-sharing chains along the c -direction that are linked within the ab -plane by Mn2-pyramid dimers. Within an ionic description, the very different local coordination of Mn1 and Mn2 results in different formal valencies of these two sites, namely $4+$ ($3d^3$) for Mn1 and $3+$ ($3d^4$) for Mn2 [13].

As a function of temperature, YMn_2O_5 undergoes a sequence of phase transitions, which demonstrate the strong coupling between the magnetic and FE order: Upon

cooling, a transition from paramagnetic to high-temperature incommensurate (HTIC) antiferromagnetic (AFM) occurs at $T_1 = 45$ K [14]. At $T_2 = 39$ K the AFM order becomes commensurate (C) with $\mathbf{q}_C = (1/2, 0, 1/4)$ [14–16] and a finite \mathcal{P} appears [17]. Upon further cooling, low-temperature incommensurate (LTIC) AFM order sets in at $T_3 = 19$ K with $\mathbf{q}_{LTIC} = (0.48, 0, 0.29)$ [14, 18], which is connected to a sign change and a reduction in magnitude of \mathcal{P} [17].

Recently, we have shown for this material that the spin-dependent Mn-O hybridization is a fundamental ingredient for the magnetically driven ferroelectricity [8]. We reached this conclusion by tracking the diffraction peaks at \mathbf{q}_C and \mathbf{q}_{LTIC} by RSXS at the Mn $L_{2,3}$ - and O K edges. In this article we present additional details of our RSXS studies [8] and elaborate on the origin of the magnetic scattering process at the O K edge.

2 Experimental

The YMn_2O_5 single crystals used for our study were grown using the PbO-PbF₂ flux method [19] and characterized by specific heat, magnetization and x-ray diffraction measurements, which were all in excellent agreement with previously published results [20, 11, 12]. For the RSXS experiments, a YMn_2O_5 sample with a (201)-surface normal was polished using 0.1 μm diamond films. Experiments were performed at the UE46-PGM1 beamline of BESSY II at the Helmholtz-Zentrum Berlin and the X1A2 beamline at the NSLS, Brookhaven National Laboratory. The former setup realizes a horizontal scattering experiment with variable incoming polarization and is equipped with a photodiode point detector. The scattering plane of the NSLS-chamber was vertical and the incoming polarization horizontal. In this case, two-dimensional cuts in reciprocal space were recorded using a Princeton Instruments PI-MTE CCD. In each case, the sample was cooled using a liquid helium cryostat.

3 RSXS lineshapes

To study the resonant scattering in the C-phase, we performed so-called $\theta 2\theta$ -scans at different photon energies, E , across the Mn $L_{2,3}$ and O K edges at UE46. We fitted each $\theta 2\theta$ -scan with a Lorentzian squared peak shape plus a linear background. The left and right panel of Fig. 1 show the resonance at the O K - and Mn $L_{2,3}$ edges, respectively, with the main resonance features marked by vertical lines.

The peak positions obtained from Bragg's law: $2d \sin \theta = \lambda$, for different E are shown by solid lines in Figs. 1 (a,d). Therein $d = 2\pi/|\mathbf{q}|$, θ and $\lambda = hc/E$ are the spacing corresponding to \mathbf{q} , the Bragg angle and the wavelength corresponding to E , respectively. At resonance, the peak center [dotted lines in Figs. 1 (a,d)] in angle space deviates from the trend which is expected according to Bragg's law due to the change of the index of reflection at the resonant energies [21, 22].

Since YMn_2O_5 has a longer correlation length of the magnetic structure than the limited penetration depth in the soft x-ray region, the width of the reflection at a given energy is given by the probed sample volume, i. e., the probing depth. Indeed the E dependent peak width gives a good measure of the x-ray absorption (XAS) cross section [Figs. 1 (b,e)]. This method provides the same bulk sensitivity as the conventional fluorescence yield measurements of the XAS, but without any self-absorption corrections. Since we are interested in the scattered intensity per volume of the resonating ions, we normalized the integrated areas, $I_{\theta 2\theta}$, at each E point by the probing volume, which we can estimate from the peak widths. $I_{\theta 2\theta}(E)$ at the O K edge has a strong resonant enhancement at the inflection point of the XAS

($E_1 = 529.7$ eV) [Figs. 1(b,c)]. Furthermore we observed a shoulder on the main peak and a second smaller peak, which is similar to Ref. [23]. At the Mn $L_{2,3}$ edges, $I_{\theta 2\theta}(E)$ has as well strong resonant enhancements at the inflection points of the XAS corresponding to the Mn L_{3-} ($E_2 = 641.3$ eV) and the Mn L_2 edges ($E_4 = 652.6$ eV) [Figs. 1(e,f)]. Surprisingly the main resonance at the Mn L_3 edge ($E_3 = 644.3$ eV) is not at an inflection point but rather at the center of the corresponding XAS peak. This complex structure of the line shape is governed by the two different crystallographic positions of Mn in YMn_2O_5 , i. e., Mn1 and Mn2, and is in very good agreement to other detailed RSXS studies on YMn_2O_5 [24].

For the Mn $L_{2,3}$ edges, we compare the peak intensity, I_{peak} , measured at the positions defined by Bragg's law to $I_{\theta 2\theta}$ [Fig. 1(f)]. It can be observed that both quantities exhibit different lineshapes and, in particular, display a different ratios of $I(E_3)$ (Mn L_3) and $I(E_4)$ (Mn L_2), the so-called branching ratio. The data presented in Fig. 1 therefore shows that just measuring the intensity at a single \mathbf{q} -point corresponding to Bragg's law [lines in Figs. 1(a,d)] does not reflect the energy dependence of the integrated intensity for two reasons: (i) the deviation of the peak position from Bragg's law at the resonances due to the change of the index of reflection; (ii) the increasing peak width at the resonance due to the smaller penetration depth (absorption effect) which moreover reduces the probing volume. These effects need to be considered for a detailed analysis of RSXS lineshapes.

4 Temperature Dependence

To accurately obtain the full integrated intensity in the 3D reciprocal space, $I_{3\text{D}}$, we used the CCD area detector at X1A2. As a function of temperature, $I_{3\text{D}}$ at E_3 (Mn L_3) tracks the neutron scattering signal [Fig. 2(a)]. Hence we are sensitive to the magnetic structure of the Mn-sites. In contrast to this, $I_{3\text{D}}$ measured at E_1 (O K)

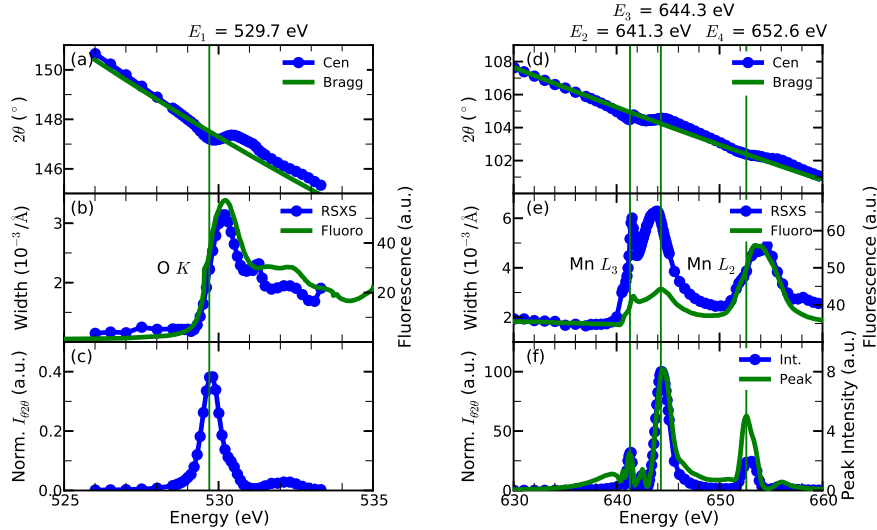


Fig. 1. Energy dependent peak center (a,d), width (b,e) and integrated intensity (c,f) of $\theta 2\theta$ -scans at $(1/2, 0, 1/4)$ in YMn_2O_5 at the O K - (a-c), and Mn $L_{2,3}$ edges (d-f) at 30 K. The incoming light (π) and the b -axis were in the scattering plane. The centers are compared to the theoretical value by Bragg's law (a,d). The fluorescence (b,e) was measured at 8 K. The peak intensity (f) was obtained by a fixed \mathbf{q} -scan.

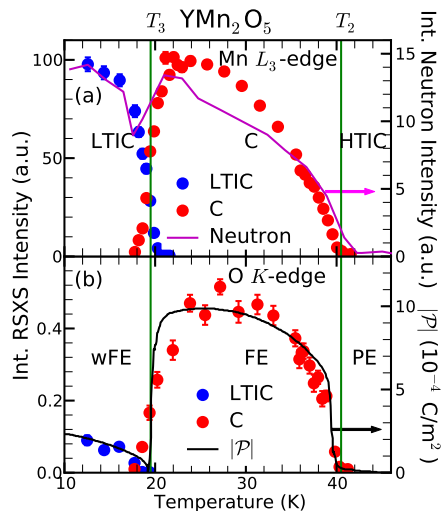


Fig. 2. Temperature dependence of the soft x-ray integrated intensity as measured at the Mn L_{3-} (a) and O K edges (b). The commensurate and incommensurate peaks could be clearly distinguished and have a coexisting phase around T_3 . Good agreement is seen with the reported (solid lines) integrated intensity observed by neutron diffraction data (a) [14] and magnitude of the electric polarization $|\mathcal{P}|$ (b) [17], respectively. The phases are low temperature incommensurate (LTIC) weak ferroelectric (wFE), commensurate (C) ferroelectric (FE) and high temperature incommensurate (HTIC) paraelectric (PE).

tracks the magnitude of the FE polarization, $|\mathcal{P}|$ [Fig. 2 (b)]. In order to establish these relationships, the correct determination of I_{3D} was very important [8]. For example, I_{peak} at the Mn L_3 edge does not recover the same intensity in the LTIC-phase as in the C-phase, in contrast to I_{3D} . This was even more critical for the O K edge, where capturing the full integrated intensity was essential to establish the proportionality of the oxygen superstructure and $|\mathcal{P}|$.

The peak positions at the Mn $L_{2,3-}$ and O K edges coincide for all determined temperatures and are in good agreement with the reported positions by neutron scattering [14–16,18]. Thanks to the high resolution and high count rate of the peak, there was no problem to distinguish the C- and LTIC-peak in the coexisting phase (Fig. 2).

5 Origin of the RSXS at the O K edge

The spin magnetic moments of the O $2p$ states are expected by theory to be only of the order of $0.01 \mu_B$ and are not refined by neutron scattering experiments. Therefore the finding of a magnetic signal from the O K edge by RSXS, which probes the modulation of the unoccupied O $2p$ states, is surprising. Especially, when one takes into account that the sensitivity to spin moments at a K edge is usually very small. The conclusion that it is indeed magnetic scattering at the O K edge was based on the same azimuthal dependence in the C-phase [23] and the same peak position even through the C-LTIC phase transition at the O K - and Mn $L_{2,3}$ edges [8].

The origin of the magnetic signal at the O K edge can be understood in terms of an orbital magnetic moment transferred to the oxygen via strong hybridization between the Mn $3d$ and O $2p$ states, in agreement with previous X-ray magnetic circular dichroism measurements (XMCD) on related transition metal oxides [25,26]. Moreover, a similar conclusion was drawn in a previous resonant elastic x-ray scattering (REXS) study at the Ga K edge on UGa_3 [27]. We therefore conclude that the intensity measured at the O K edge, directly reflects the hybridization between Mn and O. The data in Fig. 2 therefore implies that the Mn-O hybridization depends strongly on the spin structure and that this hybridization plays a role for the ferroelectric polarization.

6 Summary

In summary, we have shown that measuring $\theta 2\theta$ -scans at different photon energies enables to obtain the correct RSXS lineshapes, which is essential for the detailed analysis of the spectroscopic information contained in these data. Further, we demonstrated that the integrated peak intensities can be efficiently and accurately measured using CCD-area detectors. In the present case, this was vital for establishing the relation of the RSXS intensity to the magnetic and FE order parameter. The magnetic signal measured at the O K edge is attributed to a transferred orbital moment at O due to a strong Mn-O hybridization. The observed T -dependence hence implies that the spin-dependent Mn-O hybridization plays an important role for the multiferroicity of YMn_2O_5 .

7 Acknowledgement

Many thanks to the organizers of the REXS 2011 conference in Aussois and to Gerry Lander for helpful discussions. We thank J.-E. Hamann-Borrero and H. Wadati for their help with the experiments at UE46, and D. S. Coburn, W. Leonhardt, W. Schoenig and S. Wirick for technical support at X1A2. S.P. and J.G. thank the DFG for the support through the Emmy Noether Program (Grant GE 1647/2-1). Work performed at BNL was supported by the US Department of Energy, Division of Materials Science, under contract No. DE-AC02-98CH10886.

References

1. Sang-Wook Cheong and Maxim Mostovoy, *Nat Mater*, **6**, 13 (2007)
2. Daniel Khomskii, *Physics*, **2**, 20 (2009)
3. T. Kimura, T. Goto, H. Shintani, K. Ishizaka, T. Arima, and Y. Tokura, *Nature*, **426**, 55 (2003)
4. N. Hur, S. Park, P. A. Sharma, J. S. Ahn, S. Guha, and S-W. Cheong, *Nature*, **429**, 392 (2004)
5. Chenjie Wang, Guang-Can Guo, and Lixin He, *Phys. Rev. Lett.*, **99**, 177202 (2007)
6. A. S. Moskvin and S.-L. Drechsler, *Phys. Rev. B*, **78**, 024102 (2008)
7. Gianluca Giovannetti and Jeroen van den Brink, *Phys. Rev. Lett.*, **100**, 227603 (2008)
8. S. Partzsch, S. B. Wilkins, J. P. Hill, E. Schierle, E. Weschke, D. Souptel, B. Büchner, and J. Geck, *Phys. Rev. Lett.*, **107**, 057201 (2011)
9. A. S. Moskvin and R. V. Pisarev, *Phys. Rev. B*, **77**, 060102 (2008)
10. Th. Lottermoser, D. Meier, R. V. Pisarev, and M. Fiebig, *Phys. Rev. B*, **80**, 100101 (2009)
11. Simone Quezel-Ambrunaz, Félix Bertaut, and Georges Buisson, *C. R. Acad. Sc. Paris*, **258**, 3025 (1964)
12. Makoto Tachibana, Keita Akiyama, Hitoshi Kawaji, and Tooru Atake, *Phys. Rev. B*, **72**, 224425 (2005)
13. S. C. Abrahams and J. L. Bernstein, *J. Chem. Phys.*, **46**, 3776 (1967)
14. Isao Kagomiya, Hiroyuki Kimura, Yukio Noda, and Kay Kohn, *J. Phys. Soc. Jpn.*, **70(A)**, 145 (2001)
15. Yukio Noda, Hiroyuki Kimura, Youichi Kamada, Toshihiro Osawa, Yosikazu Fukuda, Yoshihisa Ishikawa, Satoru Kobayashi, Yusuke Wakabayashi, Hiroshi Sawa, Naoshi Ikeda, and Kay Kohn, *Physica B*, **385-386**, 119 (2006)
16. C. Vecchini, L. C. Chapon, P. J. Brown, T. Chatterji, S. Park, S-W. Cheong, and P. G. Radaelli, *Phys. Rev. B*, **77**, 134434 (2008)
17. Y. Noda, Y. Fukuda, H. Kimura, I. Kagomiya, S. Matumoto, K. Kohn, T. Shobu, and N. Ikeda, *J. Korean Phys. Soc.*, **42**, 1192 (2003)

18. P. G. Radaelli, C. Vecchini, L. C. Chapon, P. J. Brown, S. Park, and S-W. Cheong, *Phys. Rev. B*, **79**, 020404 (2009)
19. Barbara M. Wanklyn, *J. Mater. Sci.*, **7**, 813 (1972)
20. Akinobu Ikeda and Kay Kohn, *Ferroelectrics*, **169**, 75 (1995)
21. Maurizio Sacchi, Coryn F. Hague, Luca Pasquali, Alessandro Mirone, Jean-Michel Mariot, Peter Isberg, Eric M. Gullikson, and James H. Underwood, *Phys. Rev. Lett.*, **81**, 1521 (1998)
22. Jens Als-Nielsen and Des McMorrow, *Elements of Modern X-ray Physics* (John Wiley & Sons Ltd, 2001)
23. T.A.W. Beale, S.B. Wilkins, R.D. Johnson, S.R. Bland, Y. Joly, T.R. Forrest, D.F. McMorrow, F. Yakhou, D. Prabhakaran, A.T. Boothroyd, and P.D. Hatton, *Phys. Rev. Lett.*, **105**, 087203 (2010)
24. R. A. de Souza, U. Staub, V. Scagnoli, M. Garganourakis, Y. Bodenthin, S.-W. Huang, M. García-Fernández, S. Ji, S.-H. Lee, S. Park, and S.-W. Cheong, *Phys. Rev. B*, **84**, 104416 (2011)
25. E. Pellegrin, L. H. Tjeng, F. M.F. de Groot, R. Hesper, G. A. Sawatzky, Y. Moritomo, and Y. Tokura, *J. Phys. IV France*, **7(C2)**, 405 (1997)
26. E. Goering, A. Bayer, S. Gold, G. Schütz, M. Rabe, U. Rüdiger, and G. Güntherodt, *Europhys. Lett.*, **58**, 906 (2002)
27. D. Mannix, A. Stunault, N. Bernhoeft, L. Paolasini, G. H. Lander, C. Vettier, F. de Bergevin, D. Kaczorowski, and A. Czopnik, *Phys. Rev. Lett.*, **86**, 4128 (2001)